

Lawrence Berkeley National Laboratory

Lawrence Berkeley National Laboratory

Title

The structure of a-C: What NEXAFS and EXAFS see

Permalink

<https://escholarship.org/uc/item/1953r63d>

Author

Diaz, J.

Publication Date

2008-09-05

Peer reviewed

The structure of a-C: What NEXAFS and EXAFS see

J. Díaz*,¹ O. Monteiro,² and Z. Hussain³

¹*Departamento de Física, Universidad de Oviedo,
Avenida de Calvo Sotelo s/n, Oviedo-33007, Spain.*

²*Plasma Physics Laboratory, Lawrence Berkeley National Laboratory, 1, Cyclotron Road, Berkeley, CA 92740*

³*Advanced Light Source, Lawrence Berkeley National Laboratory, 1, Cyclotron Road, Berkeley, CA 92740**

(Dated: 6th July 2006)

The extended x-ray absorption spectra (EXAFS) of hard (ha-C) and soft (sa-C) amorphous carbon films were analyzed and compared to their respective Near edge x-ray absorption spectra (NEXAFS). The analysis agreed with the model originally proposed by Comelli et al.¹ where a rigid phase, the only visible by EXAFS, coexisted with a random carbon matrix. Such a rigid phase had bond lengths similar to those of diamond in the ha-C films, and to graphite in the sa-C. The proportion of atoms in atomic environments visible by EXAFS was of about 35% in both films. The empirical relation between σ^* energy and bond length appeared applicable to a-C after comparing the bond lengths obtained from the EXAFS spectra with the respective NEXAFS spectra. The structure of the random matrix was deduced from the NEXAFS spectra assuming such a relation. It was also used to determine the proportion of sp^3 bonded atoms in the a-C films which was 48% for the ha-C films and 10% for the sa-C films. These values were in agreement with the EXAFS results but very different from the obtained based in the π^*/σ^* ratio. This indicated that the intensity of the π^* band in these films, whose π bond conjugation was negligible, was lower than in π conjugated materials for the same concentration of π bonded atoms. The analysis by EXAFS spectroscopy of the annealing of the hard amorphous carbon films up to 950° C showed a gradual reduction of the first neighbor interatomic distance with increasing temperature, with no evidence of two different atomic environments, “diamond-like” and “graphite-like”, coexisting with different interatomic distances. This results supports a model where the formation of diamond-like bonds in a-C starts from a graphite-like structure under compressive strain.

PACS numbers:

I. INTRODUCTION

Amorphous carbon (a-C) is a material very much appreciated mostly because its mechanical properties. It can be as hard as diamond but, at the same time, retain an elasticity closer to alumina or wolfram. These properties depends on the detailed atomic structure of the specific a-C. Their mechanical hardness is usually associated to their concentration of sp^3 hybrids or tetrahedrally bonded atoms, and therefore, it can be tuned changing this concentration. The state of the art in the deposition techniques of a-C in the form of thin films is now enough advanced to produce very dense a-C with estimated sp^3 concentrations of the order of 80%. Such a-C films exhibit hardness and Young modulus values not too distant from those of diamond. The characterization of the a-C structure is very important to test the different structural models that describe them and being able to explain and predict new properties and ways to produce this kind of material. Several techniques have been dedicated to understand the structure with notable success. Most of them shows the structure of a-C as a mixture of single bonded atoms or sp^3 hybridized, and double bonded atoms or sp^2 hybridized. These techniques are, to name a few, Nuclear Magnetic Resonance^{2,3}, UV Raman spectroscopy⁴, X-ray Photoemission spectroscopy (XPS)^{5,6} and Electron Energy Loss

spectroscopy (EELS)⁷⁻⁹, if using electrons as a probe, or NEXAFS if using photons^{1,10,11}. EELS or NEXAFS have been the most used technique to determine the proportion of sp^3 bonded atoms since hard amorphous carbon films were produced⁷. This is because the unoccupied π^* states, only present in double bonds, are well separated in energy from the single bond states or σ^* states. Nevertheless, such a separation is not neat and some π^* states overlap at higher energies with those of the σ^* states leading to a discussion in the community about how to identify these states to count with accuracy the proportion of double bonded atoms in the films^{12,13}. The problem is more complicated because the extension and intensity of these states depends on the kind of π bonding, namely, the degree of π bond conjugation. Actually, EELS or NEXAFS spectra contains more information about the chemical structure of amorphous carbon than the simply derived from the intensity ratio of the π^* and σ^* states. It has been empirically demonstrated in organic molecules whose σ bonds are well localized that the excitation energy of their σ^* states depends on their bond length¹⁴. Using a simple model, this happens because σ bonds in this kind of molecules can be described as a potential well for the bonding electrons due to their localized character. Therefore, their energy excitations should be a function of the width of the well, i.e., the bond length. For instance, the position of the σ^* peak

with a bond length like that of diamond (1.54 Å) should be at about 291 eV, 297 eV for graphite (1.42 Å) and 310 eV (1.20 Å) for triple bonded carbon atoms. This kind of empirical relation has been also applied for the analysis of a-C films justified by the fact that disorder favors the local character of the σ bonds^{10,13}. However, it does not work when there is strong bond interaction, as it happens when atoms are π bond conjugated. But π bond conjugation in amorphous carbon is easily identified because the splitting of the σ^* excitations is well known^{10,14}. In a previous work¹⁰, we analyzed the NEXAFS spectra of ha-C films using a functional fitting assuming as valid the dependence in energy of the σ^* excitations with the carbon bond length, and also identifying the effect of π bond conjugation in the σ^* states by annealing the films up to 900° C. The present work compares such an analysis of the NEXAFS spectra of ha-C and sa-C films with the bond lengths obtained from the analysis of their EXAFS spectra. The main difference between NEXAFS and EXAFS spectra is the excitation energy of the core level electrons. This is lower than 50 eV in the NEXAFS region, making that the excited electrons interact more with the valence electrons. In the EXAFS region of the absorption spectra, the excited electrons have more energy and the resulting spectra can be well approximated by their elastic scattering with the atoms of the a-C lattice. Previous EXAFS analysis on sputtered hydrogenated a-C¹ showed that EXAFS was sensitive only to those atomic environments that were less disordered and mechanically more stiff because the EXAFS amplitude from the rest of the environments were too much dumped. However, since NEXAFS is sensitive to the electronic bonding orbitals, it should include in their spectra everything, i.e., what EXAFS sees and what it does not see. The validity of the empirical relation between the energy of the σ^* states and the bond length in a-C was tested in two a-C films with different sp^3 concentrations by comparing the bond lengths obtained from the analysis of the EXAFS spectra with the structure of the NEXAFS spectra. The checked validity of this relation permitted to extract the structure of the part of the spectra invisible by EXAFS and, therefore, obtain a method to analyze the structure of a-C using only the NEXAFS spectra.

II. EXPERIMENT

a-C thin films with different hardness were prepared by cathodic arc deposition in a preparation chamber with a base pressure of 10^{-7} mbar. The hardest samples (ha-C) were deposited on a silicon substrate pulsed biased to -100 V using a cathodic arc plasma source combined with a 90° bent magnetic macro-particle filter¹⁵. To prepare the softer a-C (sa-C) films, the silicon substrate was pulsed biased to -2000 V. The thickness of these samples was of 70 nm. The hardest sample had a hardness of about 90 GPa, close to that of diamond (100 GPa for diamond) and a Young modulus of about 400 GPa, less

than half that of diamond (1050 GPa). More details of the deposition method and properties of the samples are described elsewhere¹⁶.

The preparation chamber was physically separated from the analysis chamber. The transfer of the films to the analysis chamber was made in a locked chamber kept at low vacuum pressure (10^{-3} mbar) to avoid the a-C films to be exposed to air.

The EXAFS spectra were done in beam line 9.3, in the Materials Science endstation at the ALS¹⁷. The base pressure of the analysis chamber was 5×10^{-9} mbar, and it was never higher than 5×10^{-8} mbar during annealing. Temperature was monitored with a calibrated silicon detector pyrometer. The a-C films were annealed at increasing temperatures in different steps from 350° C till 950° C. Sample temperature was kept constant for 15 minutes at each annealing step. EXAFS spectra were measured after each annealing step. All samples formed the “magic angle”, 54.7°, to the x-rays to avoid intensity absorption dependence on the polarization of the x-rays¹⁴, except a highly oriented pyrolytic graphite (HOPG) crystal, used as a reference, that was mounted normal to the incident x-ray beam. Samples were previously cooled down by liquid nitrogen immediately after annealing to avoid temperature widening of the spectroscopic lines.

The NEXAFS spectra were calibrated in energy using the exciton of graphite at 291.65 eV. The EXAFS spectra extended up to 800 eV, which was the limit of photon energy covered by the x-ray monochromator. This meant that the useful range in k -space extracted from the EXAFS spectra was up to $k = 11$. Nevertheless, the EXAFS oscillations were practically dumped above such an energy. All the absorption spectra were taken in total electron yield (TEY) detection mode by measuring the secondary electron current to ground. This TEY signal was normalized to the incident beam intensity obtained from the TEY collected from a clean Si surface. This data treatment is often obliterated in many of the published NEXAFS spectra of a-C. Carbon contamination is common in any synchrotron beamline. It reduces the intensity of the x-ray beam at the energies of the C K edge. Normalization of the beam intensity using a gold grid, typically used for beam intensity monitoring in most of the beamlines, can create artifacts in the spectra due to the different electron yield response of Au compared to amorphous carbon^{10,14}. To have a proper x-ray absorption spectrum of a-C, normalization of the beam intensity must be done with a material that has a similar electron yield response like Si has, for instance.

III. RESULTS AND DISCUSSION

A. NEXAFS

Figure 1 shows the NEXAFS spectra of a ha-C and a sa-C film obtained before annealing. The spectra have

two main features, the sharp π^* peak at about 285 eV, and the broad σ^* structure centered at about 298 eV. Both spectra were normalized to the same intensity at 340 eV. The difference between both spectra displayed in figure 2 shows the expected lower intensity of the π^* peak of the ha-C, but it also signifies its higher intensity at the lower excitation energy of the σ^* structure.

Annealing reduces the proportion of sp^3 bonded atoms and graphitizes a-C, i.e., bonds between carbon atoms become π conjugated^{1,5,10,11}. The spectra of sa-C and ha-C annealing up to temperatures where sp^3 concentration was practically vanished are showed in figure 3. The changes observed in the NEXAFS spectra of the ha-C films are summarized in figure 4 where the spectrum of a ha-C film annealed up to 950° is subtracted from the spectrum of the as prepared film. The region at 290 eV was notoriously depressed with a clear protuberance at about 292 eV. The broad peaks at 306 eV and at 328 eV are clearly visible.

Figures 2 and 4 indicate that the empirical relation between σ^* energy and bond length used in saturated hydrocarbons should work in a-C. Most of the intensity in the σ^* region of figure 2 is at the low energy region, the excitation energy for carbon atoms with diamond-like bond lengths, in agreement with the expected higher proportion of sp^3 atoms of the ha-C film. And figure 4 shows that the same σ^* region is depressed, as supposed if annealing reduces the concentration of sp^3 atoms in a-C. It also shows well defined peaks at 292 eV and 306 eV, caused by the splitting of the σ^* band due to π bond conjugation.

The application of the empirical linear relation between bond length and σ^* bond energy in the analyzed a-C films is also justified by the expected local character of their σ bonds caused by their strong disorder. A way to determine the degree of disorder in a-C is to check the excitation energy and intensity of the multiple scattering peak which is at about 327 eV in diamond and at 329 eV in graphite. Since the origin of this peak is attributed to multiple scattering from distant neighbors^{10,18,19}, its intensity scales proportionally to the degree of order of the carbon structure²⁰. This peak is at about 322 eV and it is barely visible in any of the as prepared films. Annealing increases the order in the film and reduces the bond length. The effect of this changes in this peak is illustrated in figure 4 where this peak clearly increased its intensity and shifted its excitation energy to about 328 eV.

All the spectra were fitted using gaussian functions following the method described in a previous work¹⁰. The number of gaussian functions were the minimum to adjust all their features. They were 4 for the σ^* band and 2 for the π^* band. Figures 1 and 3 shows some of the fitted spectra together with the fitted functions. A gaussian step was added in all the spectra to take into account the excitations to the continuum of final states¹⁴. Its position was defined by the vacuum level of the analyzed surface deduced previously by photoemission, which was similar

to graphite: 4.6 eV above the Fermi level¹⁰. The result of the fits were similar to the obtained previously¹⁰. These results will be presented here in a different way based in the features obtained in figures 2 and 4, with the purpose of highlighting the differences between the ha-C and the sa-C films and also determine the degree of π conjugation of their π bonds. The σ^* band was divided in two parts: one formed by the two components centered at the lowest energy and the other defined by the other two components with higher energies. If there was not π conjugated bonds, the first part would be associated to those C-C bonds with the longest bond lengths (diamond-like) and the second part with C-C bonds of shorter bond lengths (graphite-like). Figure 5 compares the high energy part of the σ^* band of the spectrum of the as prepared ha-C and sa-C films as well as for the spectra of the same films after annealing them at different temperatures. The shape of this part of the σ^* band is very similar in any of the as prepared a-C films: it is an asymmetric function skewed toward higher energies, which reaches the highest intensity at about 296 eV. This energy would correspond to C-C bond lengths similar or a bit longer than in graphite. It can be admitted that part of the intensity of this region is due to conjugation effects from the bond interaction between the σ bonds which give rise to the low energy σ^* band. However, the intensity of this part of the spectrum is higher than the rest of the σ^* band whereas in saturated hydrocarbons with a splitting of their σ^* band due to σ -conjugation, have their higher energy σ^* resonance much weaker in all the cases¹⁴. In addition, the EELS spectrum of amorphous diamond obtained from C₆₀ under high pressure showed most of its intensity at about 291 eV, with no comparable intensity at 300 eV²¹. It is important to notice that this region of the spectrum was featureless in both kind of as-prepared a-C films. Only for high enough annealing temperatures, the σ^* peak centered at 306 eV caused by π bond conjugation got significant intensity. These annealing temperatures above which π bond conjugation was important were 650°C in the ha-C films and 500°C in the sa-C films. Therefore, the level of π bond conjugation in the as prepared sa-C and ha-C films was negligible, even if there were π bonded carbon atoms as it is proved by the presence of the π^* excitation. The reason that π bond conjugation is so poor in these a-C films is probably caused a strongly distorted bonding geometry since bond interaction due to π bonding is reduced or even killed if the number of neighbors is small²⁰ or the bonding geometry is very distorted. For instance, π bonding conjugation is minimal in the cyclo-octatetraene (C₈H₈) because its non planar geometry²².

The low energy part of the σ^* band, displayed in figure 6 was not featureless. The spectra of the as-prepared films distinguished two components. The component centered at 288.5 eV was associated to strained sp^3 bonded atoms¹⁰ like in the cyclopropane molecule because its excitation energy and sharpness was similar to the found in the NEXAFS spectrum of such a molecule²². The

other component centered at about 291 eV can be the contribution from sp^3 bonded atoms, because the bond length associated to such a σ^* excitation energy, and from sp^2 bonded atoms with π bond conjugation. Figure 6 shows that the contribution from these sp^2 bonded atoms was not important until the films were annealed to high enough temperatures. Therefore, this part of the spectrum can be associated almost integrally to sp^3 bonded atoms for the as prepared films. Its intensity was clearly much higher in the ha-C films, reflecting the result already showed in figure 2, what remarks the low concentration of sp^3 bonded in the sa-C films.

The contribution from unoccupied π states is not concealed to the very visible π^* peak but extends with significant intensity to higher excitation energies, as it is observed in other π bonded systems like graphite²³, benzene²⁴ or C_{60} ²⁵. Therefore, the intensity from π^* states was represented by two components, one at the sharp π^* peak, and the other broader and centered at about 287 eV. Figure 7 shows the π^* part of the spectra of the as prepared and after annealing ha-C and sa-C films. It is surprising how similar in intensity and shape is this part of the spectra in both kind of films. The figure shows that it changes substantially in intensity in both films after annealing them to the temperature where π bond conjugation became important.

The intensity of the π^* excitations relative to the intensity of the σ^* peak is regularly taken as a measure of the quantity of sp^3 bonded carbon atoms in the films, since only double bonds causes the π^* excitation. This ratio was compared with the same ratio measured in the spectrum of C_{60} , which is 100% sp^2 bonded and it has not long range order, therefore comparable to the analyzed a-C samples^{10,14}. This method yielded 55% of sp^3 hybridized atoms in the ha-C and 48% for the sa-C of figure 1. The percentage of sp^3 hybrids was 70% and 60% respectively if the sp^3 proportion was calculated using only the intensity of the π^* peak at 284.5 eV, to compare with other published a-C films that used that method.

The previous sp^3 estimations were done assuming that the π bonds in the as prepared films were similar to those of the used sp^2 reference, C_{60} in this case. However, it was pointed out previously that the π bond conjugation in the as prepared films was not significant. Therefore, the π bonding in both kind of materials is different, questioning if the π^* intensities from both materials are comparable. Figure 8 shows the change with temperature of the relative intensity of the π^* component respect to the intensity of the high energy σ^* band component for the sa-C and ha-C films. This ratio increased with temperature in both films but more significantly in the sa-C films. If this increase was caused by the presence of σ^* states related to sp^3 atoms in the high energy σ^* band component, it should be observed more in the ha-C film because it had a higher concentration of sp^3 atoms. Therefore, it should be attributed to changes in the π^* band. Likely, annealing and π bond conjugation made p orbital pairing more efficient. It has already shown by

photoemission spectroscopy in a-C films that their density of states at the Fermi level, which is related to the π band, increases significantly with annealing reaching densities much higher than in graphite.

The division of the σ^* band in σ^* states from sp^2 and sp^3 leads to another way to count sp^3 concentrations in as prepared a-C. It can be assumed that the proportion of σ^* states related to sp^3 atoms in the high energy part of the σ^* band in sa-C is negligible because the intensity of its low energy σ^* band is very small. Therefore, its high energy σ^* band is totally related to states from sp^2 bonded atoms. The ratio between its π^* band and its high energy σ^* band can be taken as a reference to determine the intensity from sp^3 related states in the high energy σ^* band of the ha-C films. Once this intensity is determined, the proportion of sp^3 σ^* related states with respect to the total intensity of the σ^* band gives directly the proportion of sp^3 atoms. The concentrations so obtained were about 48% for the ha-C films and 10% for the sa-C films, very different than the obtained from the previous methods in the case of the sa-C, probably because the intensity of the π^* band in these films is not comparable with that of other π conjugated materials. The difference in sp^3 concentration between both films using this other method is more in agreement with the different mechanical properties found between both films

Note that the total intensity of the NEXAFS spectra of the as-prepared ha-C films was higher than that of the sa-C films. This occurred even when the films were annealed, as it can be seen comparing the spectra in figures 1 and 3. This indicates a higher density of unoccupied states in the ha-C than in the sa-C films which could be consequence of the higher mass density of the former films. The lower total NEXAFS intensity of the sa-C suggest that its structure should be less compact than that of the ha-C, i.e, its bond length distribution should be wider than that of the ha-C. This is coherent with the way both films were deposited: given the much higher kinetic energy of the impacting carbon during the sa-C film growth, a larger quantity of defects was expected in it.

The peak at 322 eV in the as prepared films echoed the different NEXAFS intensity between both films. Figure 9 shows how this peak changes in intensity and excitation energy in each kind of film with the annealing temperature. This peak is related to multiscattering effects and, therefore, its intensity depends on the degree of disorder of the atoms in it, so the wider is the atom distribution, the weaker is its intensity. This is why the intensity of the peak increased with the annealing temperature. Also, its position in energy has to do with interatomic distances and bond angles: large distances and bond angles corresponds to low photon excitation energies. Therefore, the wide bond angle and length distribution of both films explains why its excitation energy at room temperature was so downshifted (322 eV) in both films with respect to diamond (327 eV) or graphite (329 eV). The peak approached the same excitation energy than the observed in

graphite with the annealing temperature. Note that the peak in the sa-C reached 328 eV at a lower temperature than in the ha-C, and that the photon energy of this peak was sensitively higher in sa-C even after the highest annealing temperature of the ha-C. This will be important when the analysis of the NEXAFS spectra were compared with the EXAFS results of the same films.

The low intensity of the multiscattering peak as well as its low excitation energy compared to graphite gives another good reason to state that the level of π conjugation in both films was significantly small, despite the presence of π bonds in them, clearly identified in both films by the π^* peak. Moreover, recent calculations of the graphite NEXAFS spectrum observed that the splitting of the σ^* resonance and the multiscattered peak were intimately related²⁰. Therefore, the nature of π bonding in these films is different than the found in graphite or C⁶⁰, for instance. These π bonds could correspond to sp^2 sites forming pairs in between sp^3 hybrids, as it has been proposed in several models and analysis like Raman spectroscopy^{4,12,26}, but also to sp^2 structures where π bond conjugation was frustrated because strong distortions in their lattice. *See Fig*

B. EXAFS

Figure 10 shows the EXAFS spectra of a ha-C and a sa-C thin film, before annealing, and a HOPG crystal, this last spectrum was reduced its original amplitude three folded to scale with the spectra of the a-C films.

The EXAFS spectrum of the a-C films had a significant lower amplitude than that of graphite. It is also noticeable some intensity at the oxygen K-edge (531 eV) indicating traces of oxygen contamination, which was always less than 2% the intensity of the carbon K-edge. This oxygen contamination was more important in the spectra of the soft a-C and it was probably caused by adsorption at the surface of the films. Unfortunately, oxygen and other light atoms like nitrogen are specially annoying for the analysis of the EXAFS spectra of a-C since their absorption K edges lay in the middle of the carbon EXAFS oscillations. The use of thermal annealing or ion bombardment to remove these impurities were avoided because such treatments destroys the original structure of the analyzed a-C films¹. The option chosen was mathematically filter the signal produced by the oxygen K edge extracting the signal coming from the carbon K edge EXAFS. To do so, the AUTOBK routine was used²⁷. This routine calculates the background of EXAFS spectra eliminating those frequencies below a certain cutoff in R -space after applying the Fourier Transform to the EXAFS spectra represented in k -space. The representation in k -space is made through the relation between Energy and k (electron momentum):

$$k = \sqrt{\frac{E_0 - E}{\hbar}}$$

E_0 is the photon energy chose as zero in energy for the

scattered electrons. In the case of the EXAFS spectra of carbon, E_0 is at the position of the Fermi level of the a-C, i.e., at about 285 eV. The cutoff in R -space used to extract the background of the carbon K EXAFS spectra was $R = 1 \text{ \AA}$ since there are not atoms with bond lengths below 1 \AA . The background was the low frequency signal of the spectra, i.e., the one with the largest wave length in k -space. In E -space, the length of each oscillation increases with the energy because of the relation between E (Energy) and k (electron momentum). To obtain the EXAFS spectrum of oxygen, E_0 should be 531 eV, the position of its K edge. Its background would be obtained in the same way as for the C K edge, using $R = 1 \text{ \AA}$ as a cutoff. This background contains the part of the EXAFS spectrum corresponding to carbon above the oxygen K edge, since above that point in energy, so far away from the carbon K edge, the EXAFS oscillations from carbon have the lowest frequency compared to those of oxygen. Then, the EXAFS spectrum of carbon was built joining at 531 eV the background of the oxygen K edge after subtracting a constant that represented the transitions to the continuum at the oxygen K edge. This constant was calculated determining the jump between the pre-edge and the intensity at a point 40 eV far away from the oxygen K edge, after previously aligning the pre-edge. Figure 11 shows the EXAFS spectra of the sa-C before and after filtering the oxygen signal following the method described above. This method to erase the signal related to oxygen was applied only to the sa-C film before annealing. The fits of the ha-C with the oxygen background subtracted gave similar results than the raw data but the mean deviation square parameter of the fit was worse. The reason was that the oxygen K edge falls at about the same energy than one of the second neighbor oscillations in the XAFS spectrum of diamond¹⁹. As it will be shown later on, the EXAFS of ha-C resembled in fact that of diamond. Therefore, when the region at the oxygen K edge was erased, the possible contribution from carbon at that point was also neglected.

The EXAFS oscillations of the carbon K edge were isolated using the AUTOBK routine²⁷ after the spurious oxygen signal was removed from the spectra. The cutoff used in R -space to eliminate the background was $R = 1 \text{ \AA}$. The fit of the EXAFS oscillations $\chi(k)$ was done above $k_{min} = 3.8 \text{ \AA}^{-1}$ to avoid the feature at about 322 eV, which can not be accounted for by the conventional single scattering EXAFS theory^{1,19}.

Figure 12 compares the Fourier transform of the $k\chi(k)$ EXAFS signal, i.e., $\Phi(R) = F[k\chi(k)]$, of a ha-C and a sa-C films before annealing, together with that of graphite with its amplitude reduced in three. Only the $k\chi(k)$ of the sa-C had the oxygen removed. The amplitude of $\Phi(R)$ was sensitively higher in the ha-C than in the sa-C, and it is perceptible a shift in the position of the main peak centered at about 1.45 \AA in the ha-C film and at 1.25 \AA in the sa-C film, like graphite. $\Phi(R)$ is closely related to the radial distribution of atoms around the excited atom. The most intense peak is mainly caused by

the electron scattering to the first nearest neighbors. Intensity at higher R values are associated to next nearest neighbors. In this case, the intensity associated to second nearest neighbors was not totally negligible. Actually, the spectra were better fitted if two shells were used. The sa-C film and graphite have their most intense peak centered at about the same R , which are downshifted from the position of the same peak in the ha-C, indicating that the C-C bond length in the sa-C is shorter and similar than the bond length in graphite.

Fits of the spectra were done using the IFEFFIT program²⁸. The fit of the experimental $k\chi(k)$ was done from $k_{min} = 3.8 \text{ \AA}^{-1}$ up to $k = 11 \text{ \AA}^{-1}$. Two shells were used in all the fits. The limits in R space were $R = 1 \text{ \AA}$ and $R = 2.8 \text{ \AA}$.

EXAFS spectra were fitted with the function $k\chi(k)$:

$$k\chi(k) = \sum_j k \frac{N_j S_0^2 f_j(k)}{k R_j^2} e^{-2\sigma_j^2 k^2} e^{-2R_j/\lambda(k)} \sin[2kR_j + \phi_j(k)]$$

N_j was the number of atoms of j type around the absorbing atom, $f_j(k)$ was the backscattering amplitude function of atoms of type j around the absorbing species, R_j was the distance between the absorbing atom and the atom of type j , $e^{-2\sigma_j^2 k^2}$ was the Debye-Waller factor, $e^{-2R_j/\lambda(k)}$ was a mean free path term that takes into account the inelastic losses, and $\phi_j(k)$ was the total phase shift in the electron scattering. The functions $f_j(k)$, $e^{-2R_j/\lambda(k)}$ and the total phase shift $\phi_j(k)$ were calculated using the FEFF8.10 code²⁹. The parameters to fit for each shell j were the number of atoms N_j , the distance R_j and the width of the gaussian distribution represented in the Debye-Waller factor by σ_j . The parameter S_0^2 is used to correct the losses due to multi-electron excitations which are not accounted for in the elastic scattering model used to fit the spectra^{30,31}. This parameter was 0.86 after fitting the EXAFS spectrum of graphite. It was calculated assuming that the coordination in graphite was 3.

Figure 13 shows the fit of the $k\chi(k)$ of the two a-C films before annealing and graphite. The coordination and bond length to first and second neighbors deduced from the fits of all the spectra are summarized in figures 14 and 15. The distance for the first and second neighbors were staggering similar to diamond in the ha-C film and to graphite in the sa-C film. The Debye-Waller factor was identically zero in all the samples. This is normal in graphite which has a very high in-plane Debye temperature (1300°C). But it is unusual in disordered solids where the Debye-Waller factor should be important due to the supposed large mean square fluctuations in near neighbor distances, and where even a cumulant expansion of the Debye-Waller factor in powers of k should be used to include possible anharmonic terms induced by disorder³². However, note that the coordination numbers in both kind of a-C films were very low, almost unphysical: less than 2 for the ha-C film and barely 1 for the sa-C film. This behavior is similar to the found in sputtered a-C¹, and it was explained by considering the presence of two

phases or atomic environments: one was visible by EXAFS and it consisted in a stiff structure, which seems akin to graphite in the sa-C and to diamond in the ha-C. The other phase was associated to a very disordered form of carbon with such a wide distribution in bond lengths that their EXAFS oscillations were practically quenched at rather small values of $k > 4 \text{ \AA}^{-1}$.

The annealing of the sa-C films followed a similar trend than the Ar sputtered a-C films of Comelli et al.¹: the changes experience in their EXAFS spectra with increasing temperature consisted on increasing their amplitude, whereas the bond length remained almost at the same distance than in graphite. Therefore, annealing in the sa-C consisted on increasing the graphitized regions in the film. This is graphically illustrate in figure 16 where the $k\chi(k)$ and $|\Phi(R)|^2$ EXAFS spectra of the as prepared sa-C film and annealed to 700° C were matched to the EXAFS spectrum of graphite multiplying them by a constant factor.

The changes in the ha-C films with temperature differed from those of the sa-C films. Figure 17 compares the $k\chi(k)$ and $\phi(R)$ EXAFS spectra of the ha-C film before annealing and after annealing to 950°. The oscillations of the spectra clearly increased their main wave length as the temperature was increased, approaching that of graphite, showed in the background, evidencing a shortening of the bond length. There was not too much change in the amplitude of the oscillations. Actually, it was noticed that the amplitude of the spectrum taken after annealing the ha-C film to 450° C had the lowest amplitude, as it can be seen in figure 14. One of the most remarkable conclusions obtained from the fits is that only a single bond length for first nearest neighbors was needed in them. One expected possibility was the formation of two "rigid" (visible by EXAFS) atomic environments, one "diamond-like" which decreased in concentration as the temperature increased, and "graphite-like" the other, formed by progressive ordering of the "random-matrix" due to the temperature. However, the present data shows that the "diamond-like" atomic environments relax progressively to a "graphite-like" structure. Graphitization was not complete in any of the films since the coordination numbers were still lower compared to graphite.

One surprising aspect of the transformation of the "diamond-like" phase occurred in the ha-C film is some kind of "loss" in coordination after the first annealing to 450° C. This effect was observed in the two ha-C analyzed. It would mean that some of the sp^3 hybrids in the "diamond-like" environment joined the "random-matrix" phase. Another possible interpretation of this effect can be that some of the sp^3 hybrids become threefolded although with bond lengths longer than in graphite.

C. Discussion: NEXAFS and EXAFS together

The interpretation given to the low coordination found by EXAFS in the analyzed a-C films was that the signal

of the spectra came from only part of the atomic structure of a-C. On the other hand, NEXAFS should be sensitive to all kind of environments where the atoms are bonded since it depends on the electronic bonding orbitals more than in the position of the atoms, i.e., NEXAFS should include what EXAFS sees.

The estimated atomic proportion of the environments visible by EXAFS can be obtained from the coordination numbers for the first nearest neighbors deduced from the analysis of the EXAFS spectra. The ratio of this coordination number with that of diamond in the as prepared ha-C films was 37%, similar to the obtained in the sa-C films (34%) if the coordination of graphite was used instead of diamond. These proportions are low compared to the 60% found by Comelli et al.¹ in their sputtered a-C films, emphasizing the strong disorder of the analyzed films. The difference in coordination between the two kind of a-C films found by EXAFS was in agreement with the sensitively lower intensity of the NEXAFS spectra of the sa-C films.

The atomic environments to first neighbors observed by EXAFS were closer to diamond in the ha-C films and very similar to graphite in the case of the sa-C films. This was consequent with the much lower intensity at the lower energy part of the σ^* band of the NEXAFS spectrum of the sa-C films compared to the ha-C films. It also agrees with the higher sp^3 proportion obtained in the ha-C films from the σ^* band intensity, and therefore, in total disagreement with the traditional method to measure sp^3 concentrations based on the ratio between the intensity of the π^* and σ^* bands. Therefore, this part of the spectrum should be associated, partially or totally, to the σ^* states of the atomic environments seen by EXAFS in the as prepared ha-C films. The invisible to EXAFS disordered carbon phase should be related to the higher energy part of the σ^* band since this region of the NEXAFS spectra was similar in both kind of a-C films. This means that the disordered carbon matrix structure has the wide bond distribution centered at 296 eV represented by the asymmetric function of figure 5 in the as prepared films. The σ^* states associated to the atomic environments observed by EXAFS in the sa-C films should be also within this part of the NEXAFS spectrum because the low intensity in the low energy part of the σ^* band and because the σ^* energy associated with the measured bond length. Likely, the carbon atoms associated to the EXAFS amplitude should be those bonded in between fourfolded carbon atoms since they should be in a more rigid structure to be visible by EXAFS. These kind of environment should be also observed in the ha-C but, interestingly, such a second "graphite like" environment was not detected in these films even after annealing. The reason could be that the sp^3 structure was more compact than in the sa-C film in the sense that the possibly embedded sp^2 bonded atoms in such a structure were spare, whereas in the case of the sa-C films was the inverse, i.e., the sp^2 atoms were majority and the embedded sp^3 atoms were formed by very few units units.

Then, the structure of the as-prepared ha-C films deduced from the present analysis looks like a stiff skeleton formed by the environments detected by EXAFS embedded in a less rigid disordered matrix. Such a structure would match their mechanical properties which are a hardness close to diamond, given by the "stiff skeleton", with an elasticity half that of diamond caused by the "random matrix".

The annealing process in the ha-C film supports the idea that the "diamond-like" atomic environments should not be majority since it lost stability at much lower temperature than that of diamond. The EXAFS analysis is very graphical in the way the transformation of the "diamond-like" environments is produced: the bond length is gradually reduced with temperature as if the structure relaxed to graphite. It is known the release of the internal compressive stress of these a-C films with annealing temperature^{3,33} and the connection between compressive stress and sp^3 concentration. Actually, it is commonly assumed that the process that caused this compressive stress in the films are at the origin of the increasing sp^3 bonding in them. These results support those models. The atomic environment observed by EXAFS in as-prepared ha-C films could be considered as a compressed graphitic structure that overcome a certain compressive stress threshold and become "diamond-like".

There is certain controversy to describe the process by which the a-C films release their compressive stress³, because the changes in stress are big whereas the changes in the structure of the bulk observed by different techniques are apparently small. The modification of the ha-C with temperature started already at 400° C and it went more in the direction of graphitization, and consisted in a sudden reduction in atom coordination and a light decrease in bond length. These changes might have been induced by a decrease in the compressive stress of the film due to a reorganization of the "random" environments. π bond conjugation is clearly observed for annealing temperatures above 650° C in the ha-C films. Conjugation gives strength to the bonding and, therefore, the structure observed by EXAFS should be related to it. If the "random matrix" graphitized first, given its probably lower density, a graphitic component, similar to the observed in the sa-C films would appear. That was not the case, no second environment coexisted with the "diamond-like environment". This would mean that the same "diamond-like" environment observed before annealing served as the starting point for a kind of graphitic nucleation in the films. It is important to notice that even after annealing the ha-C films to 950° C, when the total sp^2 proportion deduced from the NEXAFS spectra was 100%, the bond lengths observed by EXAFS were significantly stretched compared with those of graphite (see figure 15). Actually, the energy of the multiscattering peak was clearly below the measured in the annealed sa-C (see figure 9 which was closer to that of graphite (329 eV). This could be understood noticing that the density of the ha-C films is much higher than that of graphite or the sa-C films.

The structure of the as-prepared ha-C films should be more tridimensional because the larger proportion of sp^3 bonded atoms. sp^2 bonding does not fill the space so well, what is the reason for the lower density of graphite and the ha-C films. Annealing causes the transformation of sp^3 hybrids to sp^2 plus π conjugation bonding. This should involve important structural changes. It is possible that the dense structure of the ha-C would not allow too much atom positioning in such a transformation, locking bond angles and bond lengths. π bond conjugation involves also a repulsion between atoms similar to the repulsion that keeps graphite planes distant from each other. Actually, new computer simulations include such a repulsive potential as a key element to determine a realistic a-C structure²⁶. Then, the release of strain due to bond length reduction by π bond conjugation could be restraint by this π bond repulsion. A possible consequence of this is that p -orbital overlap between atoms would be poorer than in graphite. However, note that this is not the case. In fact, not only the NEXAFS spectra showed that the films were fully graphitized. The density of states at the Fermi level in these annealed films, measured by photoemission spectroscopy, was significantly higher than in graphite^{5,10}.

IV. CONCLUSIONS

The present work analyzed the x-ray absorption spectra of two kind of amorphous films, ha-C and sa-C, with different mechanical properties to understand their atomic structure. The result of this analysis agreed with the model proposed by Comelli et al.¹ for sputtered a-C films where a phase of rigidly bonded atoms, only visible by EXAFS, coexisted with a matrix of extremely disordered carbon atoms. This conclusion was based in the low atomic coordination of the analyzed films, below physical limits, and their negligible Debye-Waller factor extracted from the analysis of their EXAFS spectra. The proportion of material in the "rigid" phase was estimated in about 37% in both kind of films. The atomic environments detected by EXAFS in the ha-C had similar bond

lengths than in diamond whereas those of the mechanically softer films sa-C were similar to those in graphite. The low energy region of the σ^* broad resonance in the NEXAFS spectra of the a-C films was clearly identified with the sp^3 or "diamond-like" bonded part of them by comparison of the results obtained from the EXAFS spectra, confirming as valid in a-C the empirical relation between C-C bond length and σ^* excitation energy. The structure of the random carbon matrix invisible by EXAFS was deduced for both films assuming such a relation and that NEXAFS was sensitive to any bonded carbon atom. This consisted in π bonded carbon with negligible π bond conjugation and with a broad distribution of bond lengths which was centered at about 296 eV, corresponding to a bond length close to that of graphite.

The identification of regions of the σ^* band with states coming from sp^3 and sp^2 atoms served as a new way to quantify the sp^3 proportion in the films. The resulted concentrations of the as prepared a-C films using this method were 48% for the ha-C films and about 10% for the sa-C films, in agreement with the results obtained by EXAFS where only graphite-like bond lengths were found. The traditional method used to count sp^3 concentrations gave only a difference of 10% in sp^3 concentrations. This would indicate that the intensity of the π^* band due to non-conjugated π bonds, like those of the analyzed a-C films, is less intense than the intensity of the same band in a π conjugated material like graphite or C_{60} .

The annealing process of the ha-C films showed that the bond length of the "diamond-like" atomic environment decreased and approached that of graphite with increasing temperature. A second "graphite-like" environment was not detected. This result agrees with the a-C models that consider that sp^3 bonding is favored by the increasing compressive strain in the films.

Acknowledgments

We acknowledge financial support by the Spanish CI-CYT with grants No. MAT99-0724 and HF/1999-0041.

* Electronic address: javidiaz@condmat.uniovi.es

¹ G. Comelli, J. Stöhr, C. Robinson, , and W. Jark, Phys. Rev. B **38**, 7511 (1988).

² H. Pan, M. Pruski, B. C. Gerstein, F. Li, and J. S. Lannin, Phys. Rev. B **44**, 6741 (1991).

³ T. M. Alam, T. A. Friedmann, P. A. Schultz, and D. Sebastiani, Phys. Rev. B **67**, 245309 (2003).

⁴ K. W. Gilkes, S. Prawer, K. W. Nugent, J. Roberston, H. S. Sands, Y. Lifshitz, and X. Shi, J. Appl. Phys. **87**, 7283 (2000).

⁵ J. Díaz, G. Paolicelli, S. Ferrer, and F. Comin, Phys. Rev. B **54**, 8064 (1996).

⁶ R. Haerle, E. Riedo, A. Pasquarello, and A. Baldereschi,

Phys. Rev. B **65**, 45101 (2001).

⁷ D. Berger, D. R. McKenzie, and P. J. Martin, Phil. Mag. Lett. **57**, 285 (1988).

⁸ P. J. Fallon, V. S. V. C. A. Davis, J. Robertson, G. A. Amaratunga, W. I. Milne, and J. Koskinen, Phys. Rev. B **48**, 4777 (1993).

⁹ C. A. Davis, G. A. J. Amaratunga, and K. M. Knowles, Phys. Rev. Lett. **80**, 3280 (1998).

¹⁰ J. Díaz, S. Anders, X. Zhou, E. J. Moler, S. A. Kellar, and Z. Hussein, Phys. Rev. B **64**, 125204 (2001).

¹¹ R. Gago, M. Vinnichenko, H. U. Jäger, A. Y. Belov, I. Jiménez, N. Huang, H. Sun, and M. F. Maitz, Phys. Rev. B **72**, 014120 (2005).

Figure 1: NEXAFS spectra of a ha-C and a sa-C films. Both spectra were normalized in intensity to 1 at 340 eV. The gaussians and the step displayed were used to fit the spectra (see the text).

- ¹² J. Robertson, *Mat. Sci. and Engineering* **R37**, 129 (2002).
- ¹³ J. T. Titantah and D. Lamoen, *Phys.Rev. B* **70**, 075115 (2004).
- ¹⁴ J. Stöhr, *NEXAFS spectroscopy*, vol. 25 of *Springer Series in Surface Sciences* (Springer-Verlag, New York, 1992).
- ¹⁵ S. Anders, A. Anders, , and I. Brown, *J. Appl. Phys.* **74**, 4239 (1993).
- ¹⁶ S. Anders, A. Anders, I. G. Brown, B. Wei, K. Komvopoulos, J. W. A. III, and K. M. Yu, *Surf. Coat. Technol.* **68/69**, 388 (1994).
- ¹⁷ Z. Hussain, W. R. A. Huff, S. Kellar, E. J. Moler, P. A. Heimann, W. McKinney, H. A. Padmore, C. S. Fadley, , and D. A. Shirley, *J. Electron Spectroscopy and Related Phenomena* **80**, 401 (1996).
- ¹⁸ L. Papagno, L. S. Caputi, M. D. Crescenzi, and R. Rosei, *Phys. Rev. B* **26**, 2320 (1982).
- ¹⁹ D. G. McCulloch and R. Brydson, *J. Phys: Condes. Matter* **37**, 4383 (1988).
- ²⁰ D. G. McCulloch and R. Brydson, *J. Phys.: Condens. Matter* **8**, 3835 (1996).
- ²¹ H. Hirai, M. Terauchi, M. Tanaka, and K. Kondo, *Phys. Rev. B* **60**, 6357 (1999).
- ²² A. P. Hitchcock, D. C. Newbury, I. Ishii, J. Stöhr, J. A. Horsley, R. D. Redwing, A. L. Johnson, and F. Sette, *J. Chem. Phys.* **85**, 4849 (1986).
- ²³ R. A. Rosemberg, P. J. Love, and V. Rehn, *Phys. Rev. B* **33**, 4034 (1986).
- ²⁴ J. L. Solomon, R. J. Madix, and J. Stöhr, *Surf. Sci.* **255**, 12 (1991).
- ²⁵ R. Schwedhelm, L. Kipp, A. Dallmeyer, and M. Skibowski, *Phys. Rev. B* **58**, 13176 (1998).
- ²⁶ N. Marks, *J. Phys.: Condens. Matter* **14**, 2901 (2002).
- ²⁷ M. Newville, P. Livins, Y. Yacoby, E. A. Stern, and J. J. Rehr, *Phys. Rev. B* **47**, 14126 (1993).
- ²⁸ M. Neville, B. Ravel, D. Haskel, J. J. Rehr, and Y. Yacoby, *Physica B: Cond. Matter* **208-209**, 117 (1995).
- ²⁹ A. L. Ankudinov, B. Ravel, J. J. Rehr, and S. D. Conradson, *Phys. Rev. B* **58**, 7565 (1998).
- ³⁰ G. Bunker and E. A. Stern, *Phys. Rev. Lett.* **52**, 1990 (1984).
- ³¹ A. Bianconi, *X-Ray Absorption: Principles, Applications, Techniques of EXAFS, SEXAFS and XANES*. (Edited by D. C. Koningsberger and R. Prins. Wiley, New York, 1988. Pages 573-662).
- ³² E. D. Crozier, J. J. Rehr, and R. Ingalls, *X-Ray Absorption: Principles, Applications, Techniques of EXAFS, SEXAFS and XANES*. (Edited by D. C. Koningsberger and R. Prins. Wiley, New York, 1988. Pages 373-442).
- ³³ A. C. Ferrari, B. Kleinsorge, N. A. Morrison, A. Hart, V. Stolojan, and J. Robertson, *J. Appl. Phys.* **85**, 7191 (1999).

AS acknowledgment

Figure 2: (a) NEXAFS spectra of a ha-C and a sa-C films and (b) spectrum resulted from the subtraction of the spectrum of the sa-C to the ha-C, compared to the spectrum of diamond (dashed line).

Figure 3: NEXAFS spectra of annealed ha-C and a sa-C films. Both spectra were normalized in intensity to 1 at 340 eV. The gaussians and the step displayed were used to fit the spectra (see the text).

Figure 4: (a) NEXAFS spectra of a ha-C film and of the same film annealed to 950°C (b) spectrum resulted from the subtraction of both spectra, compared to the spectrum resulted from figure 2 (dashed line).

Figure 5: High energy component of the σ^* band of the NEXAFS spectra of the ha-C and sa-C films annealed to different temperatures.

Figure 6: Low energy component of the σ^* band of the NEXAFS spectra of the ha-C and sa-C films annealed to different temperatures.

Figure 7: π^* band of the NEXAFS spectra of the ha-C and sa-C films annealed to different temperatures.

Figure 8: Relative intensity of the π^* respect to the high energy σ^* band component in the ha-C films (solid dots) and the sa-C films (empty dots).

Figure 9: (a) Excitation energy and (b) intensity of the multiscattering peak in the ha-C and sa-C films.

Figure 10: EXAFS spectra of graphite (divided its amplitude by three) and the as prepared ha-C and sa-C films.

Figure 11: EXAFS spectra of a sa-C films before and after filtering the part of the spectrum corresponding to the carbon EXAFS.

Figure 12: $|\Phi(R)|^2$ EXAFS spectra of graphite (divided its amplitude by three) and the as prepared ha-C and sa-C films.

Figure 13: EXAFS spectra of graphite (divided its amplitude by three) and the as prepared ha-C and sa-C films and their corresponding fits (dotted line).

Figure 14: Coordination to first and second neighbors obtained from the fits of the EXAFS spectra of the ha-C films (full and empty dots) and the sa-C films (empty triangles) annealed to different temperatures.

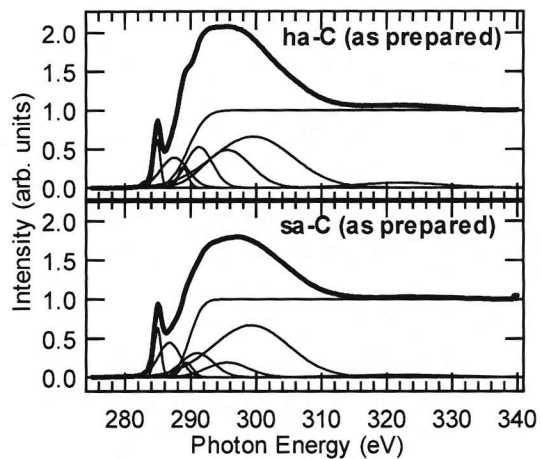


Figure 1

EXAFS1y2

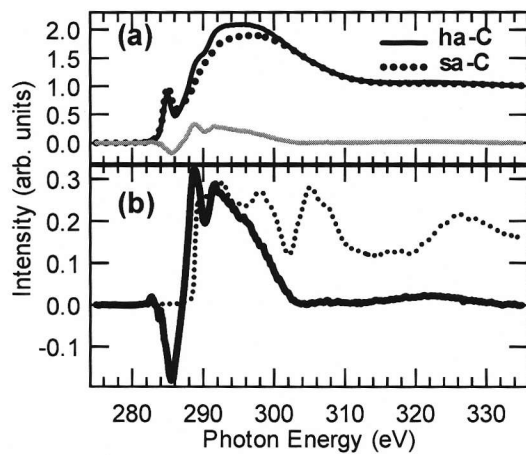


Figure 2

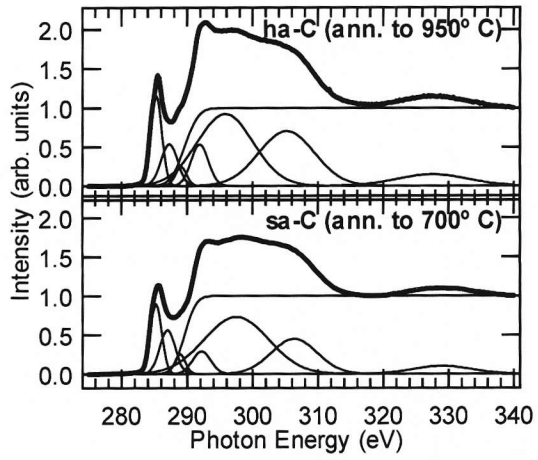


Figure 3

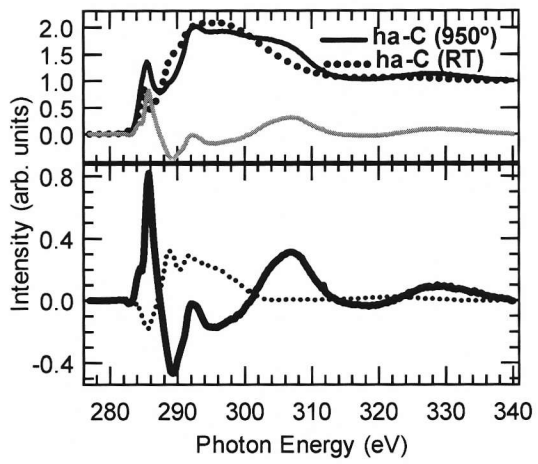


Figure 4

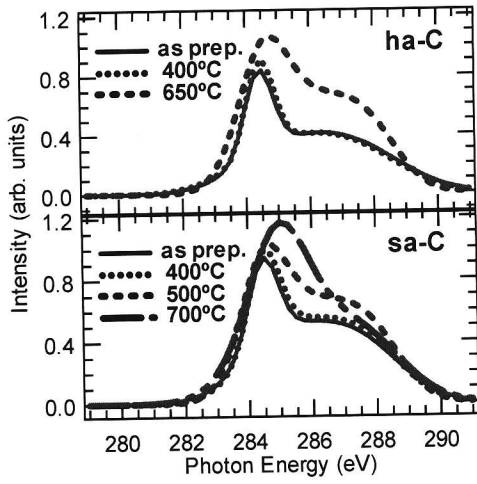


Figure 6

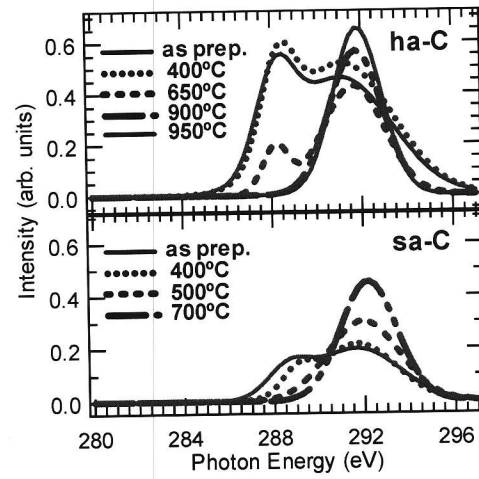


Figure 7

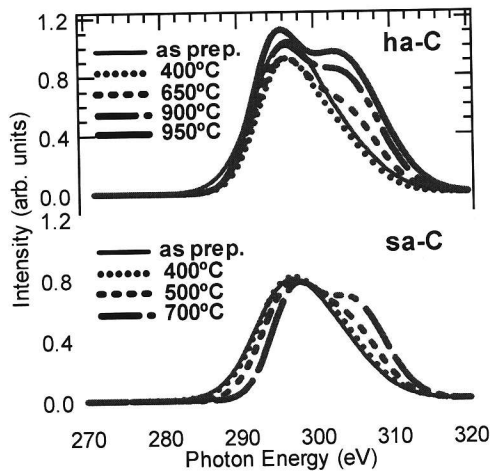


Figure 5

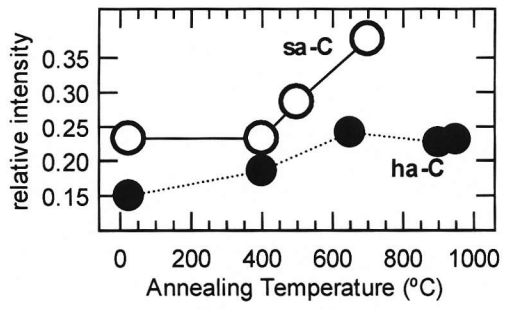


Figure 8

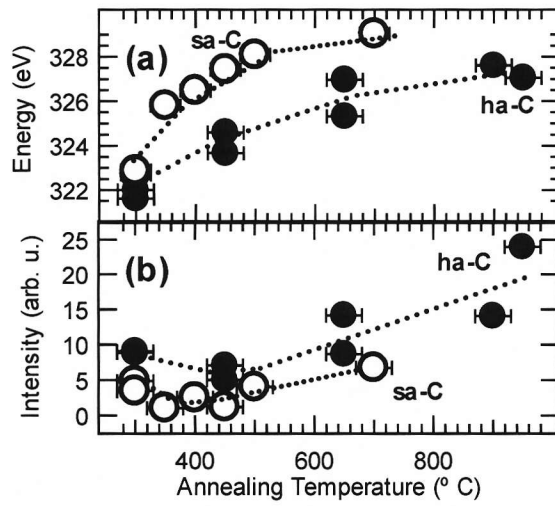


Figure 9

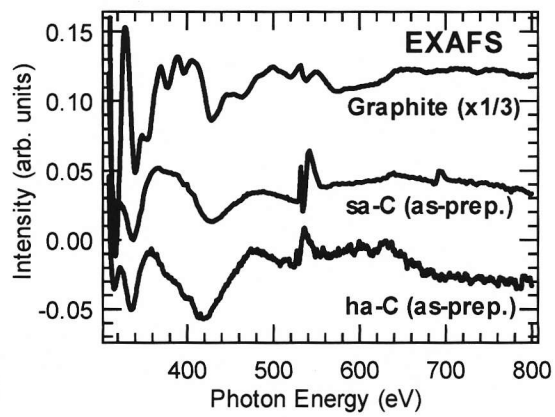


Figure 10

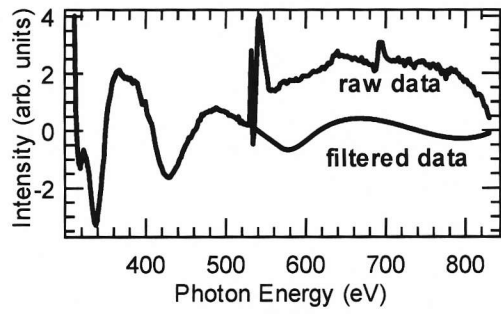


Figure 11

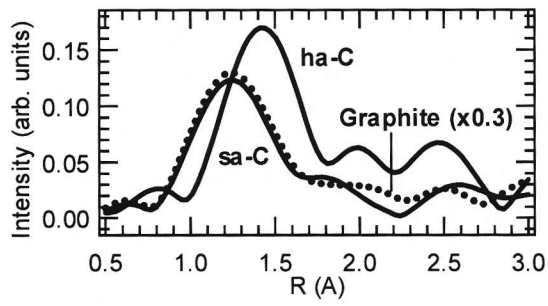


Figure 12

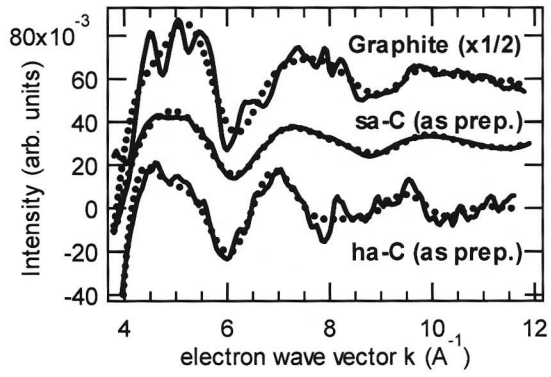


Figure 13

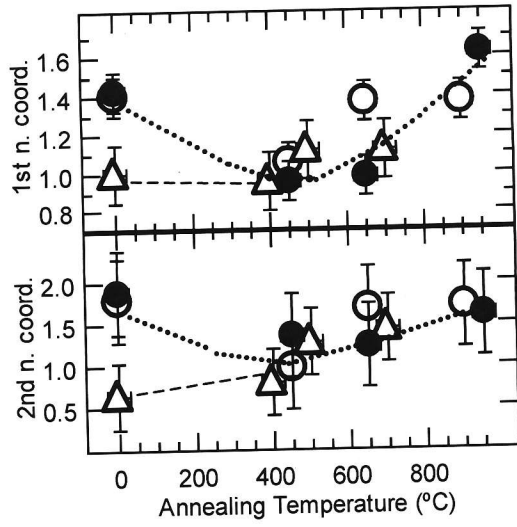


Figure 14

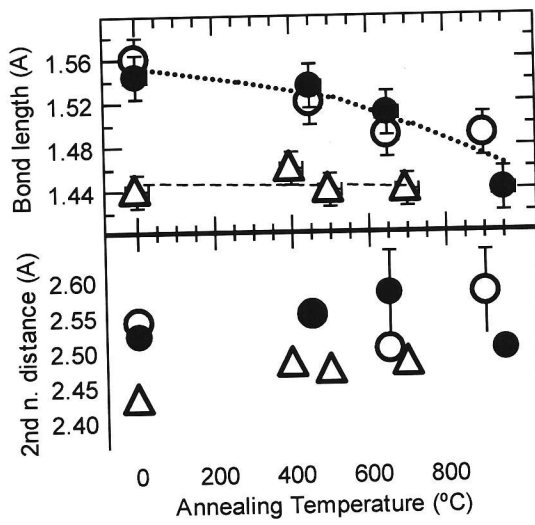


Figure 15

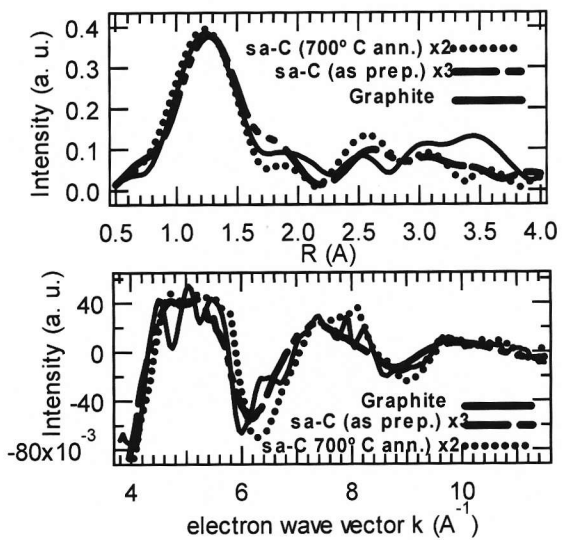


Figure 16

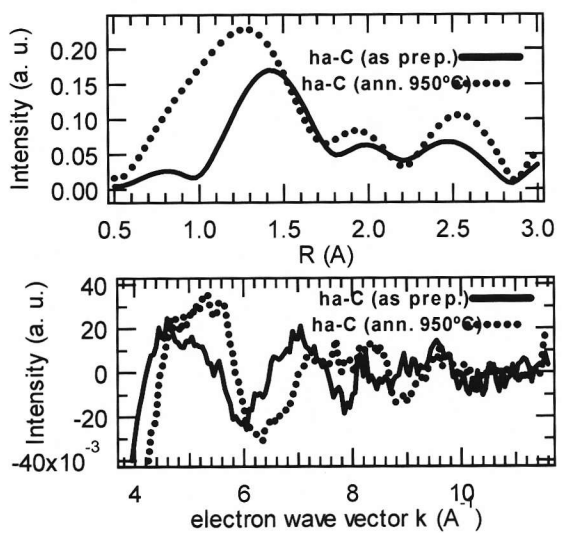


Figure 17